

Mössbauer effect probe of field-induced magnetic phase transition in $\text{LaFe}_{13-x}\text{Si}_x$ intermetallic compounds

Zhao-hua Cheng,^{a)} Nai-li Di, Qing-an Li, Zhi-qi Kou, Zhi Luo, Xiao Ma, Guang-jun Wang, Feng-xia Hu, and Bao-gen Shen

State Key Laboratory of Magnetism and International Center for Quantum Structures, Institute of Physics, Chinese Academy of Sciences, Beijing 100080, People's Republic of China

(Received 12 April 2004; accepted 6 July 2004)

Direct evidence of a field-induced magnetic phase transition in $\text{LaFe}_{13-x}\text{Si}_x$ intermetallics with a large magnetocaloric effect was provided by ^{57}Fe Mössbauer spectra in externally applied magnetic fields. Moreover, Mössbauer spectra demonstrate that a magnetic structure collinear to the applied field is abruptly achieved in $\text{LaFe}_{11.7}\text{Si}_{1.3}$ compound once the ferromagnetic state appears, showing a metamagnetic first-order phase transition. In the case of $\text{LaFe}_{11.0}\text{Si}_{2.0}$, the Fe magnetic moments rotate continuously from a random state to the collinear state with increasing applied field, showing that a second-order phase transition is predominant. The different types of phase transformation determine the magnetocaloric effects in response to temperature and field in these two samples. © 2004 American Institute of Physics. [DOI: 10.1063/1.1789235]

The discovery of a giant or large magnetocaloric effect in $\text{Gd}_5\text{Si}_2\text{Ge}_2$,¹ $\text{MnFeP}_{1-x}\text{As}_x$,² and $\text{La}(\text{Fe}_{1-x}\text{Si}_x)_{13}$ intermetallic compound³⁻⁶ gives rise to interest in searching for materials with a first-order magnetic phase transition for use as magnetic refrigerants. Previous studies indicated that the values of magnetic entropy change, $\Delta S(T)$, and adiabatic temperature change, ΔT_{ad} , for the samples with lower Si content were not only larger than those for the samples with higher Si content, but their peaks broadened asymmetrically to high temperatures.^{3,5,6} For $\text{LaFe}_{11.7}\text{Si}_{1.3}$ and $\text{LaFe}_{11.0}\text{Si}_{2.0}$, the maximum values of magnetic entropy change are 26.0 J/kg K around $T_c=185$ K and 6.0 J/kg K around $T_c=235$ K, respectively. Although it was already known from macroscopic magnetization measurements that the large values of magnetic entropy change in $\text{LaFe}_{13-x}\text{Si}_x$ compounds are associated with the first-order phase transition,^{3,4,7} the detailed phase evaluation and magnetic moment rotation in external magnetic field during the phase transition are not yet well understood. In order to elucidate the mechanism of the broadening of $\Delta S(T)$ and ΔT_{ad} peaks asymmetrically to higher temperatures, Mössbauer spectra were collected above T_c in various applied fields. In-field Mössbauer spectroscopy can give insight into understanding the connection between field-induced magnetic phase transition and magnetic entropy change above T_c from a microscopic point of view.⁸

In this letter, Mössbauer spectra in externally applied fields provide direct evidence of a field-induced magnetic phase transition in $\text{LaFe}_{13-x}\text{Si}_x$ intermetallics. $\text{LaFe}_{11.7}\text{Si}_{1.3}$ and $\text{LaFe}_{11.0}\text{Si}_{2.0}$ compounds have the cubic NaZn_{13} -type structure (Space group $Fm\bar{3}c$) with lattice constants $a=11.4865$ Å and 11.4727 Å, respectively. In hypothetical compound LaFe_{13} , Fe atoms occupy two nonequivalent sites, 8*b* site for Fe_I and 9*6i* site for Fe_{II} . La and Fe atoms form a CsCl structure. Fe_I atoms are surrounded by an icosahedron of twelve Fe_{II} atoms and Fe_{II} atoms are surrounded by nine Fe_{II} atoms and one Fe_I atom. Based on the structure, the

spectra of ferromagnetic phase should be fitted with two sextets associated with the Fe_I and Fe_{II} sites with intensity ratio of about 1:11. For $\text{LaFe}_{11.7}\text{Si}_{1.3}$ at 180 K, the values of ^{57}Fe hyperfine fields, center shifts, and quadrupole shifts are 280 ± 4 kOe, 0.02 ± 0.02 mm/s and 0.01 ± 0.02 mm/s for the Fe_I site and 254 ± 4 kOe, 0.05 ± 0.02 mm/s, and 0.00 ± 0.02 mm/s for the Fe_{II} site, respectively. However, due to the very intense absorption peak originated from the Fe_{II} atom, i.e., more than 10 times stronger than that from the Fe_I site, and a relatively small difference in hyperfine parameters between these two sites, the absorption peak is indistinguishable in the Mössbauer spectra. Since the present report focused on the magnetic-field-induced phase transition above T_c , rather than the hyperfine interactions at these two non equivalent sites, we fit the ferromagnetic phase with one sextet and the paramagnetic phase with a doublet by using average hyperfine parameters to avoid extreme complication.

Two samples with compositions of $\text{LaFe}_{11.7}\text{Si}_{1.3}$ and $\text{LaFe}_{11.0}\text{Si}_{2.0}$ were prepared by arc melting. The samples were re-melted at least six times to ensure homogeneity. The heat treatment was performed in an evacuated quartz tube at 1320 K for 45 days, and then quenched into liquid nitrogen. A single phase with the cubic NaZn_{13} -type structure was identified by x-ray diffraction patterns. Magnetization measurements were carried out with a superconducting quantum interference device magnetometer. ^{57}Fe Mössbauer spectra were recorded by a constant acceleration Mössbauer spectrometer with a $^{57}\text{Co}(\text{Pd})$ source at different temperatures and applied fields. The magnetic field up to 80 kOe parallel to γ -ray direction is provided by an Oxford Spectromag SM4000-9 superconducting split pair, horizontal field magnet system. The values of velocities and central shifts were calibrated using α -Fe foil at room temperature.

Magnetization curves show that large magnetizations are obtained above the magnetic transition. For example, Fig. 1 illustrates the magnetization curves of $\text{LaFe}_{11.7}\text{Si}_{1.3}$ and $\text{LaFe}_{11.0}\text{Si}_{2.0}$ measured above T_c at 190 and 240 K, respectively. The magnetization curve of $\text{LaFe}_{11.7}\text{Si}_{1.3}$ exhibits a very rapid increase of magnetization, M , over a narrow region of applied field, H , implying the occurrence of a spin-

^{a)} Author to whom correspondence should be addressed: electronic mail: zhcheng@aphy.iph.ac.cn

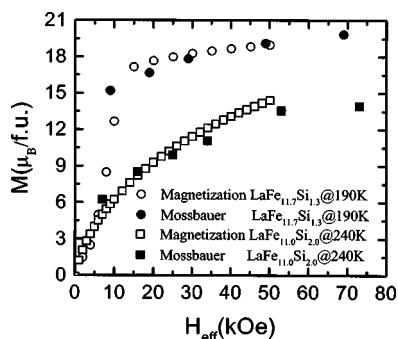


FIG. 1. Magnetization curves (open symbols) of $\text{LaFe}_{11.7}\text{Si}_{1.3}$ and $\text{LaFe}_{11.0}\text{Si}_{2.0}$ at 190 and 240 K compared with Mössbauer data (closed symbols) at the same temperature.

flip process, i.e., a metamagnetic phase transition. In the magnetization process in $\text{LaFe}_{11.0}\text{Si}_{2.0}$, it seems that the spins rotate toward the direction of the applied field and the magnetization curve fails to saturate even in an applied field of 50 kOe. Due to the step in the magnetization curve of $\text{LaFe}_{11.7}\text{Si}_{1.3}$, a large magnetocaloric response was obtained.^{3,5}

In order to demonstrate that the large increase in magnetization evident in Fig. 1 is associated with the magnetic transformation, Mössbauer spectra in various applied fields were measured for $\text{LaFe}_{11.7}\text{Si}_{1.3}$ at 190 K [Fig. 2(a)] and for $\text{LaFe}_{11.0}\text{Si}_{2.0}$ at 240 K [Fig. 2(b)], respectively. Zero-field Mössbauer spectra collected above T_c show a paramagnetic doublet owing to the quadrupole splitting. With increasing external field up to 10 kOe, no evidence of a magnetically split sextet is detected in the spectrum of $\text{LaFe}_{11.7}\text{Si}_{1.3}$, but the presence of a sextet is evident in spectrum of $\text{LaFe}_{11.0}\text{Si}_{2.0}$. With further increasing external field larger than 20 kOe, sharp well-split pairs of sextets are observed, and their areas increase rapidly at the expense of the doublets. In order to investigate the effective fields required to trigger the ferromagnetic phase, the effect of demagnetizing fields should be considered, where the effective field $H_{\text{eff}} = H_{\text{ext}} - H_{\text{demag}}$. By using magnetization data in Fig. 1 the demagnetizing fields in the direction perpendicular to the sample plane are estimated to be $4\pi M(H)$. Owing to the larger values of M for $\text{LaFe}_{11.7}\text{Si}_{1.3}$ than those of $\text{LaFe}_{11.0}\text{Si}_{2.0}$, a larger applied field is required to compensate

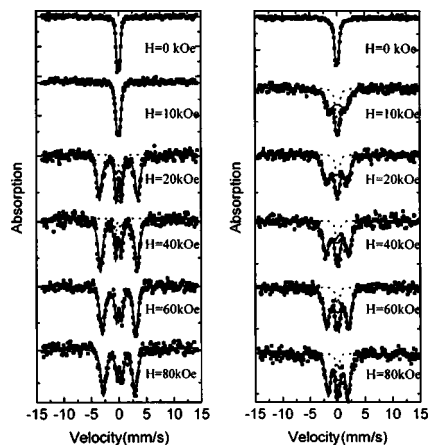


FIG. 2. Mössbauer spectra of $\text{LaFe}_{11.7}\text{Si}_{1.3}$ at 190 K (a) and $\text{LaFe}_{11.0}\text{Si}_{2.0}$ (b) at 240 K in various external magnetic fields. The dotted lines are paramagnetic subspectra.

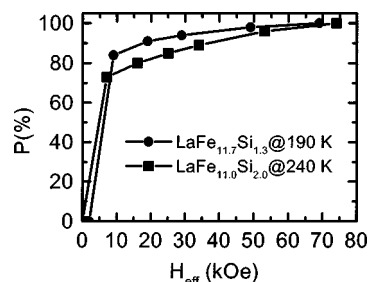


FIG. 3. Concentration of ferromagnetic component in $\text{LaFe}_{11.7}\text{Si}_{1.3}$ (closed circles) and $\text{LaFe}_{11.0}\text{Si}_{2.0}$ (closed squares) as a function of effective field.

for the demagnetizing field. By taking the demagnetizing field into account, the concentration of the ferromagnetic phase as a function of effective field was illustrated in Fig. 3. It can be seen from Fig. 3 that at effective field of about 7 kOe, the fraction of ferromagnetic component is about 80% and 70% in samples of $\text{LaFe}_{11.7}\text{Si}_{1.3}$ and $\text{LaFe}_{11.0}\text{Si}_{2.0}$, respectively, implying that the ferromagnetic component is easily triggered by magnetic field in the sample of $\text{LaFe}_{11.7}\text{Si}_{1.3}$ compound. Comparing with Gd_5Sn_4 ,⁹ a low field causes a rapid increase in the fraction of ferromagnetic component and the magnetically inhomogeneous two phases coexist over a narrow range of fields from 5 to 50 kOe.

In magnetically split spectra, the relative intensity of the second and fifth lines $I_{2,5}$ (corresponding to the $\Delta m=0$ nuclear transitions) is given by $I_{2,5} = 4 \sin^2 \theta / (1 + \cos^2 \theta)$, where θ is the angle between the magnetic moment and the external magnetic field H_{ext} (applied parallel to the γ beam direction). The spin arrangement can therefore be investigated by means of Mössbauer spectroscopy. A random Fe spin arrangement corresponds to the value of $I_{2,5}=2$. In the case when all magnetic moments are collinear to H_{ext} (i.e., for complete saturation) $I_{2,5}=0$. The disappearance of the 2–5 lines for $\text{LaFe}_{11.7}\text{Si}_{1.3}$ is obvious in Fig. 2(a) when the applied field $H_{\text{ext}} > 20$ kOe, while they are clearly present in smaller fields for $\text{LaFe}_{11.0}\text{Si}_{2.0}$ in Fig. 2(b). Figure 4(a) illustrates the intensity of the second and fifth peaks for the sextet as a function of applied field. The values of average $(\langle \cos^2 \theta \rangle)^{1/2}$, denoted as $\langle \cos \theta \rangle$ calculated from the relative line intensities $I_{2,5}$ are plotted in Fig. 4(b). It describes the rotation of the magnetic moments: $\cos \theta$ is the unit normal projection of the Fe magnetic moments in the direction of the applied field if the spatial distribution function of Fe spin directions is single peaked and reasonably narrow. For

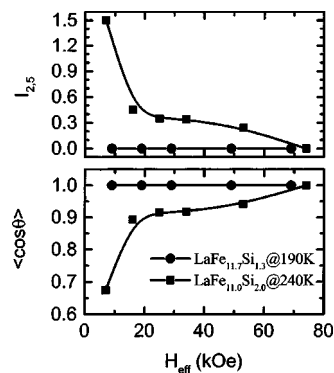


FIG. 4. Relative intensities of the 2–5 lines $I_{2,5}$ (a) and the calculated average $\cos \theta$ for $\text{LaFe}_{11.7}\text{Si}_{1.3}$ (closed circles) and $\text{LaFe}_{11.0}\text{Si}_{2.0}$ (closed squares) as a function of effective field.

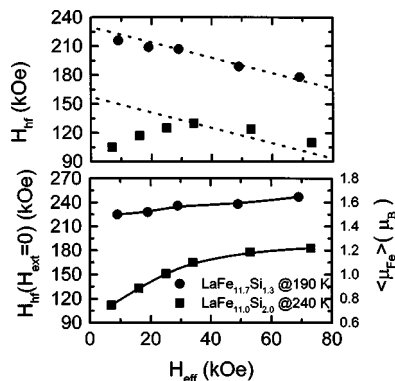


FIG. 5. Observed hyperfine field (a), induced hyperfine fields and average Fe magnetic moments (b) for $\text{LaFe}_{11.7}\text{Si}_{1.3}$ (closed circles) and $\text{LaFe}_{11.0}\text{Si}_{2.0}$ (closed squares) as a function of effective field. The dotted lines are extrapolated as expected in ferromagnetic state.

$\text{LaFe}_{11.7}\text{Si}_{1.3}$, once the applied field triggers the phase transition from the paramagnetic state to the ferromagnetic one, all magnetic moments of ferromagnetic component undergo a spin-flip process and align completely to the direction of applied field. On the other hand, for $\text{LaFe}_{11.0}\text{Si}_{2.0}$, the applied field drives the magnetic moment rotation continuously approaching the direction of applied field. When the applied field increases up to 80 kOe, all magnetic moments are completely orientated along the direction of the applied field.

To investigate the magnitude of Fe magnetic moment, the average ^{57}Fe hyperfine fields of ferromagnetic components in $\text{LaFe}_{11.7}\text{Si}_{1.3}$ and $\text{LaFe}_{11.0}\text{Si}_{2.0}$ as a function of effective field are plotted in Fig. 5(a). From Fig. 5(a), one can find two different behaviors of field dependence of ^{57}Fe hyperfine field. For the $\text{LaFe}_{11.7}\text{Si}_{1.3}$ sample, the average ^{57}Fe hyperfine fields decrease linearly with increasing magnetic field, which is consistent with that in a ferromagnetic ordered state. In contrast to $\text{LaFe}_{11.7}\text{Si}_{1.3}$, the ^{57}Fe hyperfine fields of $\text{LaFe}_{11.0}\text{Si}_{2.0}$ increase in low fields, get a maximum value at the applied field of 40 kOe, and then decrease monotonically with further increasing applied field. If we plotted hyperfine field versus applied field linearly with the same slope as that of $\text{LaFe}_{11.7}\text{Si}_{1.3}$ and extrapolated back to zero applied field, a value of 160 kOe was derived, which is very close to that of the average hyperfine field at a temperature just below T_c . In low fields the experimental data are smaller than the extrapolated data as expected in the ferromagnetic ordered state and is the result of a noncollinear magnetic structure.

It is well known that the ^{57}Fe hyperfine field, H_{HF} , is orientated antiparallel to the magnetic moment, μ_{Fe} , i.e., to the applied field with a formula $H_{\text{HF}} = A\mu_{\text{Fe}}$, where $A = 145\text{kOe}/\mu_B$ is the hyperfine coupling constant.¹⁰ Therefore, the absolute value of the average effective hyperfine field at the ^{57}Fe nucleus is given approximately by

$$\langle H_{\text{HF}} \rangle = \langle H_{\text{HF}}(H_{\text{ext}} = 0) - H_{\text{ext}} + H_{\text{demag}} \rangle = A\langle \mu_{\text{Fe}} \rangle - H_{\text{eff}}, \quad (1)$$

where the demagnetizing field $H_{\text{dem}} = 4\pi M(H)$ for the Mössbauer samples.

In the case of a highly ordered state, the magnetization is nearly saturated and the average magnetic moments do not increase significantly, therefore, the hyperfine fields decrease linearly with external magnetic field. On the other hand, if the magnetic moments are noncollinear to the applied field,

the rotation of magnetic moments results in an increase in average magnetic moment as shown in Fig. 5(b). Therefore, the hyperfine fields increase in low applied fields. With further increasing external field, the average magnetic moments approach to saturation, and the hyperfine fields thus decrease linearly with applied field.

On the basis of Eq. (1), the induced hyperfine field, defined as $H_{\text{HF}}(H_{\text{ext}}=0)$ and the average magnetic moments of Fe atom $\langle \mu_{\text{Fe}} \rangle$ were obtained and illustrated in Fig. 5(b). Using these values and taking the concentration of the ferromagnetic component into account, the total magnetization in different fields can be obtained by Mössbauer experiments according to the relation of $M(H) = nP(H)\langle \mu_{\text{Fe}} \rangle$, where n is the Fe atomic number per unit formula, P is the fraction of ferromagnetic phase as illustrated in Fig. 3. The deduced values from Mössbauer results are in good agreement with magnetization measurement (Fig. 1). The field-induced magnetic moment of Fe was clearly observed in the ferromagnetic component of $\text{LaFe}_{11.0}\text{Si}_{2.0}$, which suggests that the field results in magnetic moment rotation from the paramagnetic state (random) to the nonlinear ferromagnetic state, and then to the saturation ferromagnetic state (collinear). These results are consistent with that obtained from the intensities of the second and fifth lines of the sextets.

In summary, applied field Mössbauer spectra indicate that there are two types of field-induced magnetic phase transition in $\text{LaFe}_{11.7}\text{Si}_{1.3}$ and $\text{LaFe}_{11.0}\text{Si}_{2.0}$, respectively. $\text{LaFe}_{11.7}\text{Si}_{1.3}$ exhibits a metamagnetic phase transition above T_c . Once the ferromagnetic component appears, the spins flip to the direction of the applied field, and consequently result in a very rapid increase in magnetization over a narrow range of applied field. The metamagnetic anomaly smears out and a second-order phase transition occurs in $\text{LaFe}_{11.0}\text{Si}_{2.0}$. With increasing applied field, the magnetic moments approach continuously to the direction of applied field. The different types of phase transformation in these two samples determine the different magnetocaloric effects in response to temperature and applied field.

This work was supported by the State Key Project of Fundamental Research, and the National Natural Sciences Foundation of China. Z.H.C. thanks the Alexander von Humboldt Foundation for financial support and generous donation of some of the Mössbauer equipment used.

¹P. K. Pecharsky and K. A. Gschneidner, Jr., Phys. Rev. Lett. **78**, 4494 (1997).

²O. Tegus, E. Brück, K. H. J. Buschow, and F. R. de Boer, Nature (London) **415**, 150 (2002).

³F. X. Hu, B. G. Shen, J. R. Sun, Z. H. Cheng, G. H. Rao, and X. X. Zhang, Appl. Phys. Lett. **78**, 3675 (2001).

⁴A. Fujita, S. Fujieda, K. Fukamichi, H. Mitamura, and T. Goto, Phys. Rev. B **65**, 014410 (2001).

⁵S. Fujieda, A. Fujita, and K. Fukamichi, Appl. Phys. Lett. **81**, 1276 (2002).

⁶F. X. Hu, M. Ilyn, A. M. Tishim, J. R. Sun, G. J. Wang, Y. F. Chen, F. Wang, Z. H. Cheng, and B. G. Shen, J. Appl. Phys. **93**, 5503 (2003).

⁷H. Yamada, Phys. Rev. B **47**, 11211 (1993).

⁸F. W. Wang, G. J. Wang, F. X. Hu, A. Kurbakov, B. G. Shen, and Z. H. Cheng, J. Phys.: Condens. Matter **15**, 5269 (2003).

⁹D. H. Ryan, M. Eloneg-Jamroz, J. van Lierop, Z. Altounian, and H. B. Wang, Phys. Rev. Lett. **90**, 117202 (2003).

¹⁰I. Vincze, D. Kaptas, T. Kemeny, L. F. Kiss, and J. Balogh, Phys. Rev. Lett. **73**, 496 (1994).